Solar Energy Materials & Solar Cells 108 (2013) 225–229

Contents lists available at SciVerse ScienceDirect

Solar Energy Materials & Solar Cells

journal homepage: www.elsevier.com/locate/solmat

Materials and devices design for efficient double junction polymer solar cells

Mahbube Khoda Siddiki [a], Swaminathan Venkatesan [a], Mingtai Wang [b], Qiquan Qiao [a,*]

[a] Center for Advanced Photovoltaics, Department of Electrical Engineering and Computer Sciences, South Dakota State University, Brookings, SD 57007, USA
[b] Institute of Plasma Physics, Chinese Academy of Sciences, Hefei 230031, PR China

ARTICLE INFO

Available online 30 June 2012

Keywords:
Polymer solar cells
Single junction
Double junction
Interfacial layers

ABSTRACT

Organic solar cells exhibit potential to provide light-weight and low-cost solar energy on flexible substrates. However, current efficiency is still low for applications. New materials and device designs are needed to increase cell efficiency and make this technology available for large-scale applications. The dependence of double junction solar cell efficiency on polymer bandgaps in top and bottom subcells are presented, which provides guidance for engineering new conjugated polymers for efficient photovoltaic device development. The achievable cell efficiency can be beyond 16% with the bandgap of the bottom subcell at ~1.6 eV (~775 nm) and that of the top subcell at ~1 eV (~1240 nm). In addition, the LUMO and HOMO energy levels of the donor polymers are provided depending on various acceptor materials such as PCBM, TiO_2, ZnO and CdSe. The interfacial layers between the subcells in double junction organic devices are also discussed.

1. Introduction

Alternative energy has attracted increasing interest to mitigate dependence on conventional fossil fuels, with sunlight emerging as a particularly promising clean and readily available source. There are a number of reasons we have not yet effectively harnessed the power of the sun. Silicon (Si) solar cells usually require complex high-temperature and vacuum processing, and high purity silicon, making them cost prohibitive as an energy source [1–3]. These cells are further hampered by limited mechanical flexibility. Polymer solar cells exhibit potential as an inexpensive alternative to Si solar cells due to their solution-based processing [4,5]. Conjugated polymers also offer an attractive approach for increasing solar cell efficiencies because their bandgaps and energy levels can be engineered by modifying their chemical structure. However, efficiency of polymer solar cells does not yet approach that of inorganic solar cells. Low carrier mobilities and short carrier diffusion lengths in existing conjugated polymers make it impossible to arbitrarily increase active layer thickness in order to allow full spectrum light absorption in single junction solar cells. One promising path to increase cell efficiency is to use varied bandgaps in a serial structure in which two or more subcells with complementary absorption spectra are stacked [6–25]. In a two-terminal multijunction cell, open circuit voltage (V_{oc}) is the sum of V_{oc}'s of individual subcells, while current is determined by the minimum one in individual subcells [2,6,8,14–22,26].

Cell efficiencies have reached beyond 8% for single junction polymer solar cells, about 10% for double junction polymer cells. However, further significant increase in cell efficiency requires new design in materials and devices. Polymers currently lack appropriate bandgaps and HOMO/LUMO energy levels for optimal operation with highest efficiency in single and double junction polymer solar cells. There is a critical need for research in synthesizing and understanding a plethora of novel variable bandgap polymers with high carrier mobilities and controllable HOMO/LUMO energy levels to construct high efficiency polymer solar cells. Advances in efficiency in double junction cells also require greater fundamental understanding of interfacial layers between subcells. This work provides a guide for researchers to design and synthesize new polymers with a clear target in terms of polymer bandgaps, LUMO and HOMO energy levels, as well as selection of proper interfacial layers between subcells in a double junction device structure.

2. Results and discussion

Previous reports by Siddiki et al. [2] and Scharber et al. [27] showed that single junction polymer solar cells could achieve efficiencies up to 10–13%. Further increase in efficiency of single junction cells is challenging partly due to thermalization loss caused during the conversion from a large energy photon into an electron–hole pair in low bandgap polymers. Fortunately borrowed from the concept of inorganic solar cells [28], double

* Corresponding author.
E-mail address: Qiquan.Qiao@sdstate.edu (Q. Qiao).

0927-0248/$ - see front matter © 2012 Elsevier B.V. All rights reserved.
http://dx.doi.org/10.1016/j.solmat.2012.04.028

junction solar cell structures appear to be a promising solution to achieve a higher efficiency in polymer solar cells.

In series connection double junction solar cells, the overall current is limited by the lowest current produced from individual subcells. To maximize current output from double junction cells, the currents need to be matched between individual junctions. Current matching can also help prevent the build-up of photo-generated charges in local regions in the cells [2,6,29]. The built-up charges can lead to formation of local potential and electrical field that affect performance of double junction solar cells by deviating from the optimal power output point, thereby reducing V_{oc}, short circuit current density (J_{sc}), or fill factor (FF)

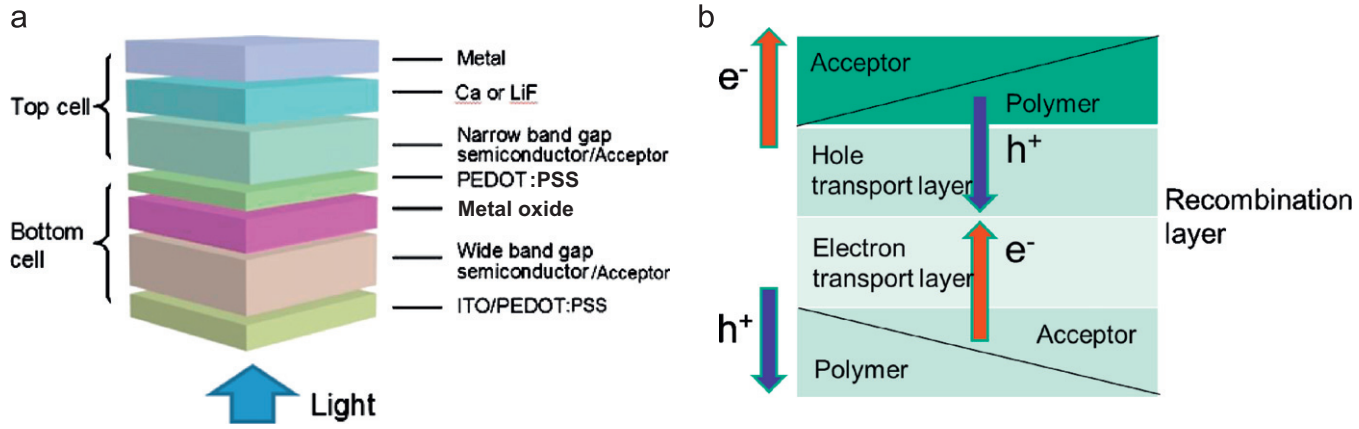

Fig. 1. (a) Device configuration of a typical double junction polymer solar cell and (b) the mechanism of the interfacial layers consisting of HTL and ETL. The HTL is typically PEDOT:PSS, while ETL is TiO_2, ZnO or Nb_2O_5.

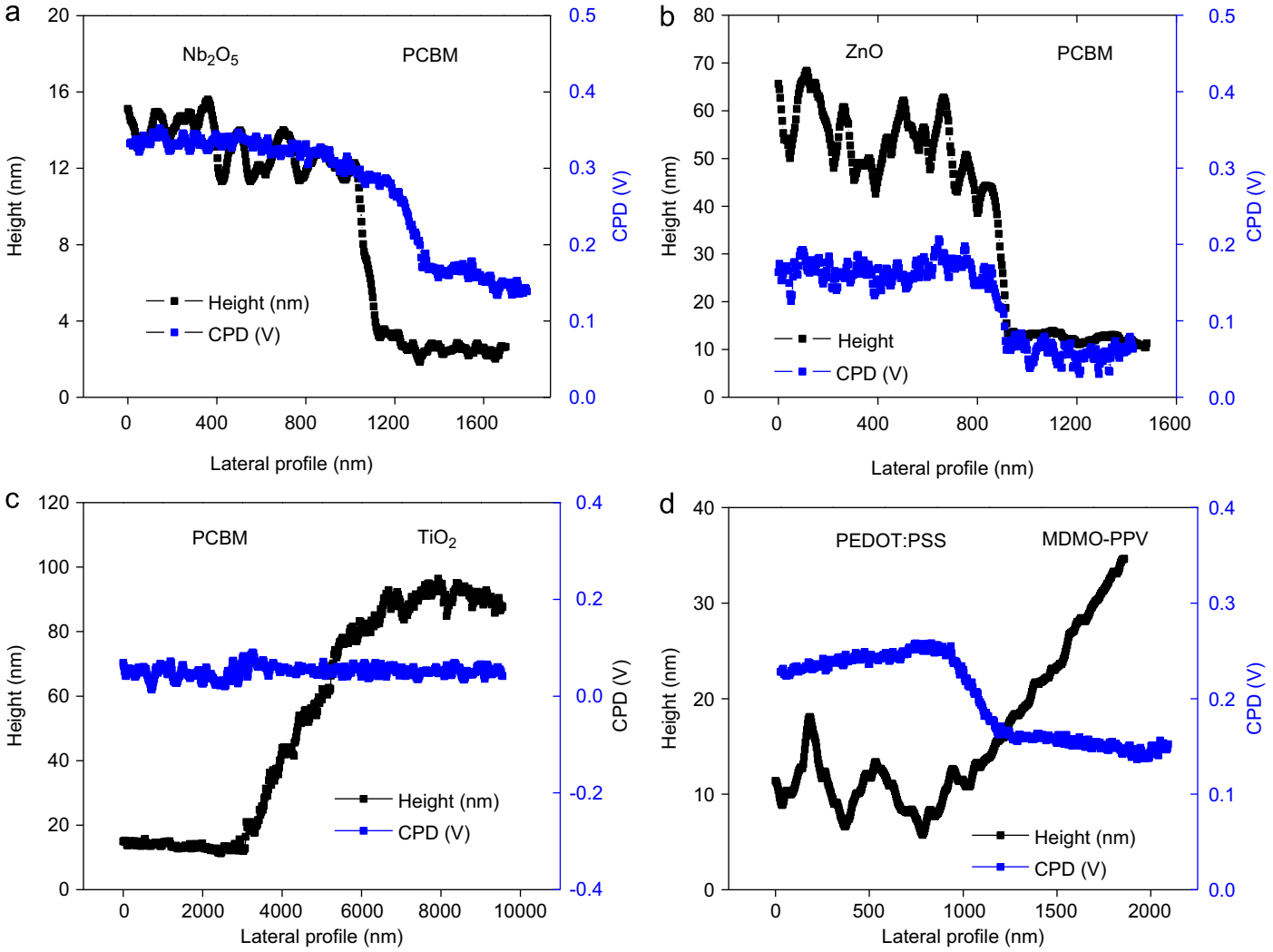

Fig. 2. Height and surface potential across a surface interface measured by scanning probe microscope (SPM) of (a) Nb_2O_5 on top of PCBM, (b) ZnO on top of PCBM, (c) TiO_2 on top of PCBM, and (d) MDMO-PPV on top of PEDOT:PSS.

[2]. Current matching can be achieved by selecting appropriate donors, varying active layer thicknesses, and/or engineering donor–acceptor morphology and compositions. The overall double junction solar cell current density ($J_{sc\text{-}double}$) in series connection is equal to the smallest one from its corresponding individual subcell. The overall open circuit voltage ($V_{oc\text{-}double}$) of double junction solar cells in series connection is the sum of V_{oc}s' of individual subcells as $V_{oc\text{-}double} = V_{oc1} + V_{oc2}$. The V_{oc1} and V_{oc2} are the open circuit voltage of respective individual subcells.

Deposition of double or multiple subcells in series can lead to formation of inverse junctions between adjacent subcells. Such inverse junctions can behave as potential barriers for charge flow from one subcell to the next. To solve this issue, interfacial layers including electron transport layer (ETL) and hole transport layer (HTL) are required to be inserted between adjacent subcells as a tunneling/recombination layer. This can also help align Fermi levels of adjacent subcells and reduce energy loss in the tunneling/recombination process, thereby minimizing the photovoltage loss of the overall double junction cells [29]. In addition to the above mentioned purpose of tunneling/recombination, the interfacial layers play two more roles: (1) a protective layer for the bottom subcell and (2) a foundation for the top subcell [2]. The interfacial layers are required to be transparent or at least semi-transparent to low energy photons because non-transparent interfacial layers block the light from arriving at the second subcell. Transparent metal oxides such as $TiO_{x(x \leq 2)}$ and ZnO were reported to serve as ETL, while poly(3,4-ethylenedioxythiophene) doped with poly(styrenesulfonate) (PEDOT:PSS) and other transitional metal oxides (e.g. V_2O_5 and MoO_3) act as HTL [2,25,30]. The interfacial layers can be prepared by spin coating (e.g. ZnO and Nb_2O_5) [11,31], dip coating (e.g. TiO_2), dc megnetron sputtering (e.g. ITO) [9], and thermal evaporation (e.g. Sn, Au, Ag, WO_3) [6,11].

Fig. 1a shows device configuration of a typical double junction polymer solar cell. The bottom subcell usually uses wide bandgap polymers, while the top utilizes narrow bandgap polymers. As mentioned above, the interfacial layers typically consist of HTL such as PEDOT:PSS and ETL such as TiO_2, ZnO and Nb_2O_5. Fig. 1b shows the operation mechanism of the interfacial layers consisting of HTL and ETL. The electrons from the top subcell transport to the overall top electrode, while the holes from the bottom one transport to the overall bottom electrode, forming current flow in the external circuit. In the meanwhile, the holes from the top subcell transfer to the HTL, while the electrons from the bottom transfer to the ETL. Such holes and electrons transport through the respective transport layer and then tunnel/recombine at the interfacial layers.

The surface potentials (or contact potential difference (CPD)) of Nb_2O_5/PCBM, ZnO/PCBM, TiO_2/PCBM and MDMO-PPV/PEDOT:PSS were studied using Agilent SPM 5500. As shown in Fig. 2, the height plots confirmed that Nb_2O_5, ZnO, and TiO_2 were deposited on top of the PCBM layer, while MDMO-PPV was deposited onto PEDOT:PSS. The surface potential (or contact potential difference (CPD)) results showed that an energy barrier of 0.25 eV existed for electron transfer from PCBM to Nb_2O_5 (Fig. 2a), while such barrier was only 0.12 eV from PCBM to ZnO (Fig. 2b). However, a very small energy barrier was observed for electron transfer from PCBM to TiO_2 (Fig. 2c). In addition, we also studied the surface potential on the PEDOT:PSS/MDMO-PPV samples and the results showed that hole transfer from MDMO-PPV to PEDOT:PSS was energetically favorable (Fig. 2d).

Fig. 3 shows the dependence of calculated overall double junction cell efficiency on the bandgaps of the polymers in the bottom and top subcells. It can be seen that the bandgaps of the bottom and top subcells need to be carefully selected within the inner regions in Fig. 3 to achieve the highest possible efficiency for double junction polymer solar cells. Fig. 4 shows the calculated photovoltaic performance of double junction polymer solar cells connected in series in terms of V_{oc}, J_{sc}, and cell efficiency (η) with a dependence on the absorption cutoff wavelength of the bottom and top subcells. The calculation was conducted with following presumptions: (1) individual subcells are connected in series, (2) each subcell absorbs equally divided amount of photon flux and generates identical current density,

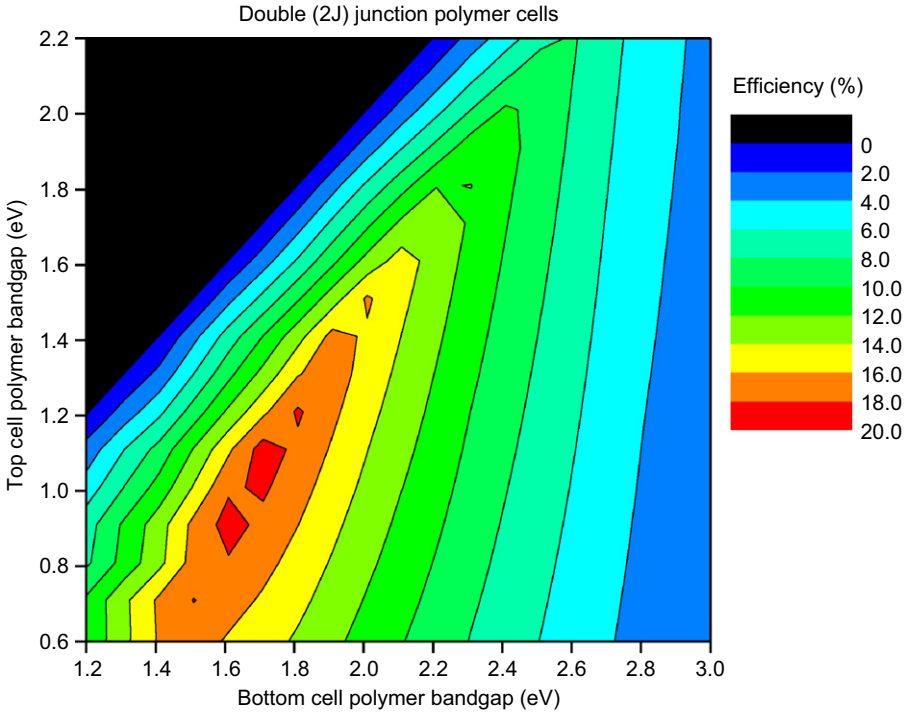

Fig. 3. The dependence of calculated overall double junction cell efficiency on polymer bandgaps in the bottom and top subcells.

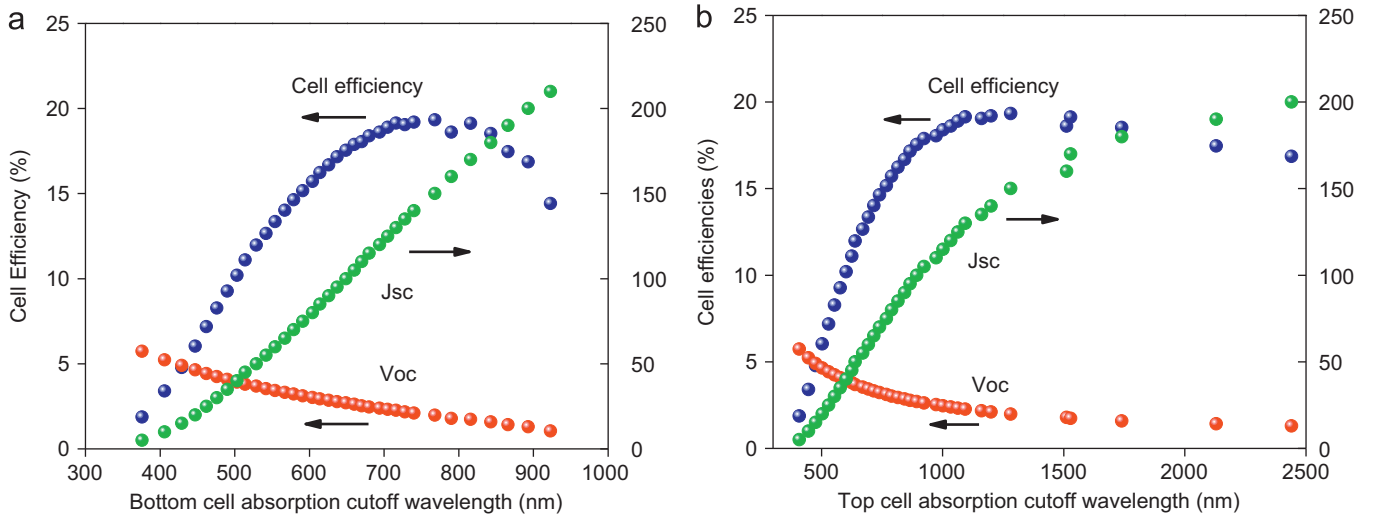

Fig. 4. The calculated photovoltaic performance of double junction polymer solar cells connected in series in terms of V_{oc}, J_{sc}, and η with a dependence on the absorption cutoff wavelength of the (a) bottom and (b) top subcell.

Table 1
Polymer parameters (bandgaps, LUMOs and HOMOs) for efficient double junction polymer solar cells based on acceptors such as PCBM, TiO_2, ZnO and CdSe. The LUMOs of PCBM and CBs of TiO_2, ZnO, and CdSe were adopted from Ref. [2].It is presumed that an offset of 0.3 eV is needed for exciton dissociation.

Acceptor	Top subcell (eV)			Bottom subcell (eV)		
	Polymer bandgap	Polymer LUMO	Polymer HOMO	Polymer Bandgap	Polymer LUMO	Polymer HOMO
PCBM LUMO = −4.3 eV	~1	−4.0	−5.0	~1.6	−4.0	−5.6
TiO_2 CB = −4.4 eV	~1	−4.1	−5.1	~1.6	−4.1	−5.7
ZnO CB = −4.2 eV	~1	−3.9	−4.9	~1.6	−3.9	−5.5
CdSe CB = −3.8 eV	~1	−3.5	−4.5	~1.6	−3.5	−5.1

leading to minimal current loss, (3) the bandgap (E_g) of the donor in individual subcells is obtained from their cutoff absorption wavelengths and the V_{oc} of individual subcells was estimated by subtracting E_g from exciton binding energy (E_b), and (4) the *FF* and incident photon to current efficiency (*IPCE*) were 0.65 and 0.60, respectively. The cell efficiencies of double junction solar cells were finally calculated using the equation

$$\eta_{double} = \frac{J_{sc\text{-}double} V_{oc\text{-}double} FF}{P_{light}}.$$

As the light absorption spectrum is extended into longer wavelength (red or near infrared) regions, the polymer bandgaps decrease, which increases J_{sc} but reduces V_{oc}, as shown in Fig. 4. Therefore, a balance between J_{sc} and V_{oc} needs to be obtained so that their product along with *FF* ($J_{sc} \times V_{oc} \times FF$) is maximized. An optimal light absorption spectrum range of both the bottom and top subcells needs to be identified to achieve the highest possible efficiency. In order to maximize the overall cell efficiency, the bandgap of the bottom subcell would be at ~1.6 eV (~775 nm), while that of the top subcell at ~1 eV (~1240 nm). In addition to the bandgaps in the subcells, the absolute energy levels including LUMO and HOMO are also critical. Table 1 presents the LUMO and HOMO energy levels of donor polymers combined with various acceptor materials such as PCBM, TiO_2, ZnO and CdSe.

3. Conclusions

The materials and devices design for efficient double junction polymer solar cells are presented. An optimal light absorption spectrum range of both the bottom and top subcells in double junction cells needs to be identified to achieve the highest possible energy conversion efficiency. The achievable cell efficiency can be beyond 16% with the bandgap of the bottom subcell at ~1.6 eV (~775 nm) and that of the top subcell at ~1 eV (~1240 nm). In addition, the LUMO and HOMO energy levels of the donor polymers are provided depending on various acceptor materials such as PCBM, TiO_2, ZnO and CdSe. The interfacial layers between the subcells in the double junction organic devices are also discussed. This work may provide guidance to design and fabricate high efficiency single and double junction polymer solar cells.

Acknowledgments

The authors would like to acknowledge the partial financial support from NSF EPSCoR (EPS-EPSCoR-0903804), NSF CAREER (ECCS-0950731), NASA EPSCoR (NNX09AP67A), South Dakota BoR Competitive Research Grant program, and US–Egypt Joint Science &Technology Funds (913).

References

[1] S.-S. Sun, N.S. Sariciftci, Organic Photovoltaics: Mechanisms, Materials, and Devices (Optical Engineering), CRC Press, Boca Raton, 2005.
[2] M.K. Siddiki, J. Li, D. Galipeau, Q. Qiao, A review on polymer multijunction solar cells, Energy and Environmental Science 3 (2010) 867–883.
[3] T. Xu, Q. Qiao, Conjugated polymer–inorganic semiconductor hybrid solar cells, Energy and Environmental Science 4 (2011) 2700–2720.
[4] P. Taranekar, Q. Qiao, J. Jiang, K.S. Schanze, J.R. Reynolds, Hyperbranched conjugated polyelectrolyte bilayers for solar cell applications, Journal of American Chemical Society 129 (2007) 8958–8959.
[5] Q. Qiao, Y. Xie, J.J.T. McLeskey, Organic/inorganic polymer solar cells using a buffer layer from all-water-solution processing, Journal of Physical Chemistry C 112 (2008) 9912–9916.

[6] A. Hadipour, B.d. Boer, P.W.M. Blom, Solution-processed organic tandem solar cells with embedded optical spacers, Journal of Applied Physics 102 (2007) 074506.
[7] C.-W. Chen, Y.-J. Lu, C.-C. Wu, E.H.-E. Wu, C.-W. Chu, Y. Yang, Effective connecting architecture for tandem organic light-emitting devices, Applied Physics Letters 87 (2005) 241121.
[8] A.G.F. Janssen, T. Riedl, S. Hamwi, H.H. Johannes, W. Kowalsky, Highly efficient organic tandem solar cells using an improved connecting architecture, Applied Physics Letters 91 (2007) 073519.
[9] K. Kawano, N. Ito, T. Nishimori, J. Sakai, Open circuit voltage of stacked bulk heterojunction organic solar cells, Applied Physics Letters 88 (2006) 073514.
[10] G. Dennler, H.-J. Prall, R. Koeppe, M. Egginger, R. Autengruber, N.S. Sariciftci, Enhanced spectral coverage in tandem organic solar cells, Applied Physics Letters 89 (2006) 073502.
[11] J. Gilot, M.M. Wienk, R.A.J. Janssen, Double and triple junction polymer solar cells processed from solution, Applied Physics Letters 90 (2007) 143512.
[12] J. Yang, J. You, C.-C. Chen, W.-C. Hsu, H.-r. Tan, X.W. Zhang, Z. Hong, Y. Yang, Plasmonic polymer tandem solar cell, ACS Nano 5 (2011) 6210–6217.
[13] S. Sista, M.-H. Park, Z. Hong, Y. Wu, J. Hou, W.L. Kwan, G. Li, Y. Yang, Highly efficient tandem polymer photovoltaic cells, Advanced Materials 22 (2010) 380–383.
[14] J. Gilot, M.M. Wienk, R.A.J. Janssen, Optimizing polymer tandem solar cells, Advanced Materials 22 (2010) E67–E71.
[15] A. Hadipour, B. de Boer, J. Wildeman, F.B. Kooistra, J.C. Hummelen, M.G.R. Turbiez, M.M. Wienk, R.A.J. Janssen, P.W.M. Blom, Solution-processed organic tandem solar cells, Advanced Functional Materials 16 (2006) 1897–1903.
[16] T. Ameri, G. Dennler, C. Lungenschmied, C.J. Brabec, Organic tandem solar cells: a review, Energy and Environmental Science 2 (2009) 347–363.
[17] J. Arokiaraj, H. Okui, H. Taguchi, T. Soga, T. Jimbo, M. Umeno, High-quality thin film GaAs bonded to Si using SeS2—a new approach for high-efficiency tandem solar cells, Solar Energy Materials and Solar Cells 66 (2001) 607–614.
[18] G. Dennler, M.C. Scharber, T. Ameri, P. Denk, K. Forberich, C. Waldauf, C.J. Brabec, Design rules for donors in bulk-heterojunction tandem solar cells—towards 15% energy-conversion efficiency, Advanced Materials 20 (2008) 579–583.
[19] I.M. Dharmadasa, Third generation multi-layer tandem solar cells for achieving high conversion efficiencies, Solar Energy Materials and Solar Cells 85 (2004) 293–300.
[20] G. Ganguly, T. Ikeda, T. Nishimiya, K. Saitoh, M. Kondo, A. Matsuda, Hydrogenated microcrystalline silicon germanium: a bottom cell material for amorphous silicon-based tandem solar cells, Applied Physics Letters 69 (1996) 4224–4226.
[21] A. Hadipour, B. de Boer, P.W.M. Blom, Device operation of organic tandem solar cells, Organic Electronics 9 (2008) 617–624.
[22] N.-K. Persson, O. Inganäs, Organic tandem solar cells—modelling and predictions, Solar Energy Materials and Solar Cells 90 (2006) 3491–3507.
[23] T. Trupke, P. Wurfel, Improved spectral robustness of triple tandem solar cells by combined series/parallel interconnection, Journal of Applied Physics 96 (2004) 2347–2351.
[24] O. Hagemann, M. Bjerring, N.C. Nielsen, F.C. Krebs, All solution processed tandem polymer solar cells based on thermocleavable materials, Solar Energy Materials and Solar Cells 92 (2008) 1327–1335.
[25] D.W. Zhao, X.W. Sun, C.Y. Jiang, A. Kyaw, G.Q. Lo, D.L. Kwong, An efficient triple-tandem polymer solar cell, IEEE Electron Device Letters 30 (2009) 490–492.
[26] A. Yakimov, S.R. Forrest, High photovoltage multiple-heterojunction organic solar cells incorporating interfacial metallic nanoclusters, Applied Physics Letters 80 (2002) 1667–1669.
[27] M.C. Scharber, D. Mühlbacher, M. Koppe, P. Denk, C. Waldauf, A.J. Heeger, C.L. Brabec, Design rules for donors in bulk-heterojunction solar cells—towards 10% energy-conversion efficiency, Advanced Materials 18 (2006) 789–794.
[28] M. Stan, D. Aiken, B. Cho, A. Cornfeld, V. Ley, P. Patel, P. Sharps, T. Varghese, High-efficiency quadruple junction solar cells using OMVPE with inverted metamorphic device structures, Journal of Crystal Growth 312 (2010) 1370–1374.
[29] P. Peumans, A. Yakimov, S.R. Forrest, Small molecular weight organic thin-film photodetectors and solar cells, Journal of Applied Physics 93 (2003) 3693–3723.
[30] J.Y. Kim, K. Lee, N.E. Coates, D. Moses, T.Q. Nguyen, M. Dante, A.J. Heeger, Efficient tandem polymer solar cells fabricated by all-solution processing, Science 317 (2007) 222–225.
[31] M.K. Siddiki, S. Venkatesan, Q. Qiao, Nb_2O_5 as a new electron transport layer for double junction polymer solar cells, Physical Chemistry Chemical Physics 14 (2012) 4682–4686.